Neuroprotective Properties of Cannabigerol in Huntington's Disease: Studies in R6/2 Mice and 3-Nitropropionate-lesioned Mice

Sara Valdeolivas · Carmen Navarrete · Irene Cantarero ·
María L. Bellido · Eduardo Muñoz · Onintza Sagredo

Abstract Different plant-derived and synthetic cannabinoids have shown to be neuroprotective in experimental models of Huntington's disease (HD) through cannabinoid receptor-dependent and/or independent mechanisms. Herein, we studied the effects of cannabigerol (CBG), a nonpsychotropic phytocannabinoid, in 2 different *in vivo* models of HD. CBG was extremely active as neuroprotectant in mice intoxicated with 3-nitropropionate (3NP), improving motor deficits and preserving striatal neurons against 3NP toxicity. In addition, CBG attenuated the reactive microgliosis and the upregulation of proinflammatory markers induced by 3NP, and improved the levels of antioxidant defenses that were also significantly reduced by 3NP. We also investigated the neuroprotective properties of CBG in R6/2 mice. Treatment with this phytocannabinoid produced a much lower, but significant, recovery in the deteriorated rotarod performance typical of R6/2 mice. Using HD array analysis, we were able to identify a series of genes linked to this disease (e.g., symplekin, Sin3a, Rcor1, histone deacetylase 2, huntingtin-associated protein 1, δ subunit of the gamma-aminobutyric acid-A receptor (GABA-A), and hippocalcin), whose expression was altered in R6/2 mice but partially normalized by CBG treatment. We also observed a modest improvement in the gene expression for brain-derived neurotrophic factor (BDNF), insulin-like growth factor-1 (IGF-1), and peroxisome proliferator-activated receptor-γ (PPARγ), which is altered in these mice, as well as a small, but significant, reduction in the aggregation of mutant huntingtin in the striatal parenchyma in CBG-treated animals. In conclusion, our results open new research avenues for the use of CBG, alone or in combination with other phytocannabinoids or therapies, for the treatment of neurodegenerative diseases such as HD.

Key Words Phytocannabinoids · cannabigerol · Huntington's disease · inflammation · neuroprotection

S. Valdeolivas and C. Navarrete share first authorship.

E. Muñoz and O. Sagredo share senior authorship of this study.

S. Valdeolivas · O. Sagredo (✉)
Departamento de Bioquímica y Biología Molecular, Instituto Universitario de Investigación en Neuroquímica, Universidad Complutense, Madrid 28040, Spain
e-mail: onintza@med.ucm.es

S. Valdeolivas · O. Sagredo
Centro de Investigación Biomédica en Red sobre Enfermedades Neurodegenerativas (CIBERNED), Universidad Complutense, Madrid, Spain

S. Valdeolivas · O. Sagredo
Instituto Ramón y Cajal de Investigación Sanitaria (IRYCIS), Facultad de Medicina, Universidad Complutense, Madrid, Spain

C. Navarrete · M. L. Bellido
Vivacell Biotechnology Spain, Córdoba, Spain

I. Cantarero · E. Muñoz (✉)
Instituto Maimónides de Investigación Biomédica de Córdoba (IMIBC)/Hospital Universitario Reina Sofía, Universidad de Córdoba, Córdoba, Spain
e-mail: fi1muble@uco.es

Introduction

Huntington's disease (HD) is an inherited neurodegenerative disorder characterized by motor abnormalities, cognitive dysfunction, and psychiatric symptoms [1]. The primary cause of the disease is a mutation in the huntingtin gene, which consists of a CAG triplet repeat expansion translated into an abnormal polyglutamine tract in the amino-terminal portion of this protein that becomes toxic for striatal and cortical neuronal subpopulations [2]. At present, there is no specific pharmacotherapy to alleviate motor and cognitive symptoms and/or to arrest/delay disease progression in HD. Thus, even though a

few compounds have produced encouraging results in preclinical studies (i.e., unsaturated fatty acids, inhibitors of histone deacetylases, coenzyme Q10, minocycline), none of the findings obtained in these studies have yet led to the development of an effective medicine [3]. Importantly, following on from an extensive preclinical evaluation using different experimental models of HD (reviewed in [4] and [5]), clinical tests are now being performed with cannabinoids. Using experimental models that reproduce different cytotoxic stimuli that operate in HD pathogenesis, for example rodents treated with mitochondrial toxins (e.g., inhibitors of mitochondrial complex II), quinolinate-lesioned mice, or transgenic mice bearing mutated forms of human huntingtin, preclinical studies with cannabinoids demonstrated preservation of striatal neurons [6–11]. The beneficial effects of cannabinoids were exerted through multiple mechanisms of action, including cannabinoid receptor type 1 (CB_1) activation (e.g., excitotoxic models [8, 11]), cannabinoid receptor type 2 (CB_2) activation (e.g., inflammatory models [10]), and CB_1/CB_2-independent mechanisms. For example, cannabinoid receptor-independent effects were induced by compounds with antioxidant profiles, such as Δ^9-tetrahydrocannabinol (Δ^9-THC) and cannabidiol (CBD), and were particularly evident against the toxicity caused by the mitochondrial complex II inhibitor 3-nitropropionic acid (3NP), which primes oxidative injury [6, 7]. The combination of botanical extracts enriched in these 2 phytocannabinoids, similar to the formulation of the already approved cannabis-based medicine, Sativex® (GW Pharmaceuticals, Salisbury, UK) [12, 13], also preserved striatal neurons in rats subjected to 3NP intoxication [14], a model priming, as mentioned above, calpain activation and oxidative injury as major cytotoxic mechanisms and in which, as mentioned above, both Δ^9-THC [6] and CBD [7], administered separately, have already been found to display neuroprotective properties. These effects of the Sativex®-like combination of phytocannabinoids were also, as expected, independent of CB_1 and CB_2 receptors [14], and attributed to the inherent antioxidant properties of both phytocannabinoids that may depend on their particular chemical structure (reviewed in [15]). In addition, it has been suggested that Δ^9-THC, and especially CBD, may exert its neuroprotective effects by regulating the activity of inducible transcription factors such as nuclear factor kappa B (NF-κB), nuclear factor erythroid 2-related factor 2 (Nrf-2), and peroxisome proliferator-activated receptor (PPARγ) [16].

Cannabigerol (CBG) is another major phytocannabinoid having a pharmacological profile relatively similar to Δ^9-THC and CBD in relation to its CB-independent activities. CBG is nonpsychotropic and does not bind or activate CB_1 or CB_2 [17, 18]. However, CBG is antioxidant [17, 18], as well as anti-inflammatory, as it inhibits lipopolysaccharide-induced (LPS) release of proinflammatory cytokines and prostaglandin E2 in primary microglial cells [19], activates

PPARγ [19], and attenuates murine colitis induced by intracolonic administration of dinitrobenzene sulfonic acid [20]. CBG also targets α-2 adrenergic receptors [21], and serves as an antagonist of serotonin 5-hydroxytryptamine 1A receptors ($5HT_{1A}$) [21]. CBG has not been studied in HD but its pharmacological profile (e.g., antioxidant and activator of PPARγ) presents certain interest as a potential disease-modifying agent in this disorder. This possibility prompted us to extend our preclinical work with classic phytocannabinoids in HD to CBG using first a neurotoxin-based model, 3NP-lesioned mice. This is a model in which the death of striatal neurons is predominantly associated with the occurrence of mitochondrial dysfunction, calpain activation, and oxidative stress [14, 22]; therefore, a model in which CBG may be beneficial owing to its antioxidant and anti-inflammatory activities. Moreover, we also wanted to study CBG in R6/2 mice, a transgenic model of HD that reproduces a very aggressive pathological phenotype and that is frequently used in preclinical evaluation of potential neuroprotective compounds. Cannabinoids other than CBG are particularly active in this murine model [8, 9]. To this end, we subjected 3NP-lesioned or R6/2 mice, and their respective controls, in two separate experiments to daily treatments with CBG at a dose of 10 mg/kg. In the case of 3NP-lesioned mice, the treatments were prolonged for 4 days before the animals were euthanized and their brains collected for further analysis. In the case of R6/2 mice, treatments began at 4 weeks and were prolonged up to 10 weeks after birth, the age at which animals were also euthanized and their brains collected for further analysis. The progression of neurological deficits (e.g., failed rotarod performance, altered locomotor activity, clasping, dystonia) was recorded before (only in R6/2 mice) and/or during (in both experiments) the treatment period, whereas for the extent of the striatal damage, the brains were analyzed using different histological parameters [e.g., Nissl staining; NeuN or dopamine- and cyclic adenosine monophosphate-regulated phosphoprotein, Mr 32 kDA (DARPP-32) immunostaining; reactive microgliosis determined with Iba-1 immunohistochemistry; astrogliosis labelled with glial fibrillary acidic protein (GFAP) immunostaining], and the expression of various biochemical markers related to the endocannabinoid signaling system [e.g., CB_1 and CB_2, fatty acid amide hydrolase (FAAH) and monoacylglycerol lipase (MAGL) enzymes] or that have been found previously to be altered in different HD models [e.g., the neurotrophins brain-derived neurotrophic factor (BDNF) and insulin-like growth factor-1 (IGF-1), the glutamate transporters GLT-1 and glutamate aspartate transporter (GLAST), DARPP-32, some antioxidant enzymes, and proinflammatory enzymes and cytokines] [2, 8–10, 14, 23]. The striatal samples from both experiments were also analyzed with a specific HD polymerase chain reaction (PCR) array system. We performed an additional experiment conducted with CBG in striatal progenitor cell lines STHdh$^{Q7/Q7}$ and STHdh$^{Q111/Q111}$ expressing

endogenous wild-type and mutant huntingtin, respectively, which was aimed at determining the effects of this phytocannabinoid on PPARγ receptors (see Supplementary Information).

Materials and Methods

Animals and Treatments

All animals used in this study were housed in a room with a controlled photoperiod (08:00–20:00 light) and temperature (22±1 °C) with free access to standard food and water. All experiments were conducted according to local and European rules (European Union directive 86/609/EEC) and approved by the respective animal research ethic committees of our universities (Universidad de Córdoba and Universidad Complutense). To induce lesions of the striatum, 16-week-old C57BL/6 male mice (Harlan Ibérica, Barcelona, Spain) were subjected to seven intraperitoneal (i.p.) injections of 50 mg/kg 3NP [Sigma-Aldrich, St. Louis, MO, USA; one injection each every 12 h prepared in phosphate-buffered saline (PBS)]. 3NP-treated animals and their respective nonlesioned controls (injected with PBS) were used for pharmacological studies with CBG (THC Pharm GmbH, Frankfurt, Germany). Treatments consisted of 4 i.p. injections every 24 h with CBG at a dose of 10 mg/kg, a dose within the range of effective doses for phytocannabinoids in HD and other disorders when they were administered in pure form [8–11, 14] or vehicle (0.2 % dimethyl sulfoxide plus 5 % bovine serum albumin in PBS), with the first and the last injections 30 min before the first and the last injections of 3NP, respectively. All animals were euthanized 12 h after the last injection of 3NP. In a second experimental approach, we used a colony of R6/2 and wild-type mice generated from initial breeders obtained from Jackson Laboratories (Bar Harbor, ME, USA; code: B6CBA-Tg(HDexon1)62Gbp/1 J; 160±5 repeat expansions), which is presently available in our animal facilities. The colony was maintained by back-crossing R6/2 males with B6CBAF1/J females. Animals were subjected to genotyping to confirm the presence of the transgene with the mutated huntingtin (see details in [8] and [9]). Male R6/2 and wild-type animals were used at the age of 4 weeks after birth, an age at which motor symptoms have not appeared yet [8, 9]. Mice were treated daily with i.p. injections of CBG (10 mg/kg) or vehicle (Tween 80-saline, 1:16) up to the age of 10 weeks, at which point the animals were euthanized (always 24 ho after the last injection of CBG).

Sampling

Once euthanized, mice were dissected and their brains removed. The right hemisphere was used to dissect the striatum, which was frozen in 2-methylbutane cooled in dry ice and stored at −80 °C for biochemical analyses [quantitative reverse transcription (qRT)-PCR, enzyme activities, array system]. The left hemisphere was fixed in fresh 4 % paraformaldehyde (in 0.1 M PBS) for 36 h at 4 °C, followed by cryoprotection in 30 % sucrose and storage at −80 °C for staining and immunohistochemical analysis. In all experiments, at least 6–8 animals were used per experimental group.

Evaluation of the Neurological Deterioration

Mice were subjected to different behavioral tests for determining their neurological status. In R6/2 mice, we evaluated motor coordination in the RotaRod test, using a LE8200 device (Harvard Apparatus, Barcelona, Spain), with acceleration from 4 to 40 r.p.m. over a period of 600 s. Mice were tested on 1 day every week from week 4 of age, for 4 consecutive trials, with a rest period of approximately 20 min between trials. Data from the first trial were not used in the statistical analyses. The first RotaRod performance, at week 4, was established as basal performance. In 3NP-lesioned mice, we evaluated the motor activity (ambulation in an automated actimeter), the hindlimb clasping and dystonia, and the truncal dystonia, following previously-described procedures [24]. All behavioral tests were conducted prior to drug injections to avoid acute effects of the compounds under investigation.

Real-time qRT-PCR Analysis

Total RNA was isolated from striata using either SurePrep RNA/Protein Purification Kit (Fisher Bioreagents, Madrid, Spain) or RNeasy Lipid Tissue Mini Kit (Qiagen, Hilden, Germany). The total amount of RNA extracted was quantitated by spectrometry at 260 nm and its purity from the ratio between the absorbance values at 260 and 280 nm. After genomic DNA was removed (to eliminate DNA contamination), single-stranded complementary DNA was synthesized from up to 1 μg of total RNA using Rneasy Mini Quantitect Reverse Transcription (Qiagen) and the iScript cDNA Synthesis Kit (Bio-Rad, Hercules, CA, USA). The reaction mixture was kept at −20 °C until enzymatic amplification. In the case of samples from R6/2 mice, quantitative RT-PCR assays were performed using TaqMan Gene Expression Assays (Applied Biosystems, Foster City, CA, USA) to quantify mRNA levels for CB_1 (ref. Mm01212171_s1), CB_2 (ref. Mm02620087_s1), FAAH (ref. Mm00515684_m1), MAGL (ref. Mm00449274_m1), IGF-1 (ref. Mm00439560_m1), BDNF (ref. Mm04230607_s1), DARPP-32 (ref. Mm00454892_m1), GLT-1 (ref. Mm00441457_m1), GLAST (ref. Mm00600697_m1), tumor necrosis factor (TNF)-α (ref. Mm00443260_g1), and PPARγ (ref. Mm01184322_m1) using glyceraldehyde 3-phosphate dehydrogenase (GAPDH)

expression (ref. Mm99999915_g1) as an endogenous control gene for normalization. The PCR assay was performed using the 7300 Fast Real-Time PCR System (Applied Biosystems) and the threshold cycle (Ct) was calculated by the instrument's software (7300 Fast System; Applied Biosystems). The iQ^{TM} SYBR Green Supermix (Bio-Rad) was used to quantify mRNA levels, in samples from 3NP-lesioned mice, for cyclooxygenase (COX)-2, TNF-α, interleukin (IL)-6, and inducible nitric oxide synthase (iNOS). Real-time PCR was performed using a CFX96 Real-Time PCR Detection System (Bio-Rad). The GAPDH housekeeping gene was used to standardize the mRNA expression levels in every sample. Expression levels were calculated using the $2^{-\Delta\Delta Ct}$ method. Sequences of oligonucleotide primers are given in Table 1. The complementary DNA samples were also used for an array analysis using the RT^2 Profiler PCR Array Mouse HD (PAMM-123Z; Qiagen), which has been designed with 84 HD-related genes, following the manufacturer's instructions.

Measurement of Oxidative Stress Parameters

To determine different parameters related to oxidative stress and antioxidant systems, the right striatum obtained from 3NP-lesioned and control mice was homogenized in 0.1 M phosphate buffer (pH 7.4) using an Ultra-Turrax (IKA, Staufen im Breisgau, Germany) for 30 s on ice. Homogenates were cleared by centrifugation at 13,400 g at 4 °C and the supernatants were collected. The protein content of the samples was determined using the Bradford assay. Catalase activity was assayed by the method described by Luck [25] in which the breakdown of hydrogen peroxide (H_2O_2) is measured at 240 nm. Briefly, the assay mixture consisted of 12.5 mM H_2O_2 in 50 mM phosphate buffer (pH 7.0) and 0.05 ml of the supernatant of each striatal homogenate (10 %), and the change in absorbance was recorded at 240 nm. Enzyme activity was calculated using the millimolar extinction coefficient of H_2O_2 (0.07). The results are expressed as percentage of the mean activity in the control group. Superoxide dismutase (SOD) activity was assayed according to the method described by Kono [26], wherein the reduction of nitroblue tetrazolium chloride (NBT) was inhibited by the SOD that was measured at 560 nm spectrophotometrically. Briefly, the reaction was initiated by the addition of 20 mM of hydroxylamine hydrochloride to the mixture containing 1 mM of NBT and 0.1 ml of each striatal homogenate. The results are expressed as percentage of the mean activity in the control group. Reduced glutathione (GSH) levels in each striatal homogenate were estimated according to the method described by Ellman [27]. The tissue samples (0.1 ml) were treated with trichloroacetic acid (10 %) during 30 min at room temperature and then centrifuged at 600 g for 15 min. The supernatants were collected and incubated with 6 mM 5,5'-dithiobis(2-nitrobenzoic acid) (DTNB). DTNB and GSH react to generate 2-nitro-5-thiobenzoic acid and glutathione disulfide (GSSG). Since 2-nitro-5-thiobenzoic acid is a yellow-colored product, its determination at 412 nm is used as an index of GSH concentrations, which are represented as percentage of mean levels found in the control group.

Histological Analyses

Brains fixed in 4 % paraformaldehyde and cryoprotected in 30 % sucrose were sliced (30-μm thick) with a cryostat at the level of the caudate-putamen and collected on gelatin-coated slides for immunohistochemical analysis of 1) EM48, a marker of mutant huntingtin aggregates, using a monoclonal anti-mouse EM48 antibody (Millipore, Billerica, MA, USA) used at 1/400 (see details in [28]); and 2) DARPP-32, a marker of striatal projection neurons, using a monoclonal anti-mouse DARPP-32 antibody (Cell Signaling Technology, Danvers, MA, USA) used at 1/300. In the case of 3NP model, 5-μm-thick sections were used for Cresyl-violet staining (see details in [29]) and for immunohistochemical analysis of 1) NeuN, a marker of neurons, using a monoclonal antimouse NeuN antibody (Millipore) used at 1/100; 2) Iba-1, a marker of microglial cells, using a monoclonal anti-mouse Iba-1 antibody (Millipore) used at 1/50; and 3) GFAP, a marker of astrocytes, monoclonal antimouse GFAP antibody (Santa Cruz Biotechnology, Santa Cruz, CA, USA) used at 1/50. In all cases, sections were incubated overnight at 4 °C. After incubation with the corresponding primary antibody, sections were washed in 0.1 M PBS and incubated for 2 h at room temperature with the appropriate biotin-conjugated antirat (1:500; Millipore), biotin-conjugated antirabbit (1:300; Sigma/Aldrich, Madrid, Spain) or goat antimouse (Millipore) secondary antibodies. Reaction was revealed with the Vectastain® Elite ABC kit (Vector Laboratories, Burlingame, CA, USA). Negative

Table 1 List of mouse primer sequences used in quantitative polymerase chain reaction

Gene	Forward	Reverse
IL6	5'-GAACAACGATGATGCACTTGC-3'	5'-TCCAGGTAGCTATGGTACTCC-3'
iNOS	5'-AACGGAGAACGTTGGATTTG-3'	5'-CAGCACAAGGGGTTTTCTTC-3'
COX-2	5'-TGAGCAACTATTCCAAACCAGC-3'	5'-GCACGTAGTCTTCGATCACTATC-3'
TNFα	5'-AGAGGCACTCCCCCAAAAGA-3'	5'-CGATCACCCCGAAGTTCCCATT-3'
GAPDH	5'-TGGCAAAGTGGAGATTGTTGCC-3'	5'-AAGATGGTGATGGGCTTCCCG-3'

control sections were obtained using the same protocol with omission of the primary antibody. All sections for each immunohistochemical procedure were processed at the same time and under the same conditions. A Nikon Eclipse 90i microscope and a Nikon DXM 1200 F camera (Nikon, Tokyo, Japan) were used for slide observation and photography, and all image processing was done using ImageJ (National Institutes of Health, Bethesda. MD, USA). For this purpose, multiple sections, selected from levels located approximately 200 μm from the middle of the lesion, were obtained from each brain and used to generate a mean value per subject. In the case of the quantification of EM48 and DARPP-32 immunostaining, three 30-μm-thick slices (at a distance of 360 μm each other) per animal and 4 images at a magnification of 40× per each slice were used. The number of aggregates, or of DARPP-32-stained cells, was expressed as the mean value per field.

Cell Cultures and PPARγ Transcriptional Activity

Additional experiments were conducted in conditionally immortalized striatal progenitor cell lines STHdh$^{Q7/Q7}$ expressing endogenous wild-type huntingtin, and STHdh$^{Q111/Q111}$ expressing comparable levels of mutant huntingtin with 111 glutamines [30]. Cells were cultured in Dulbecco's Modified Eagle Medium (DMEM) (Lonza Ibérica, Barcelona, Spain) supplemented with 4 % fetal bovine serum and 4 % bovine growth serum, 2 mM L-glutamine, and antibiotics. The cells were grown at 33 °C in a humidified atmosphere containing 5 % CO_2. In 24-well plates, 10^5 cells/ml were cultured and transiently co-transfected with the expression vector GAL4-PPARγ and the luciferase reporter vector GAL4-luc using Roti®-Fect (Carl Roth, Karlsruhe, Germany) following the manufacturer's instructions. Twenty-four hours post-transfection, cells were treated with increasing concentrations of CBG for 6 h. Then, the cells were lysed in 25 mM Tris-phosphate pH 7.8, 8 mM $MgCl_2$, 1 mM dithiothreitol, 1 % Triton X-100, and 7 % glycerol. Luciferase activity was measured in the cell lysate using a TriStar LB 941 multimode microplate reader (Berthold, Bad Wildbad, Germany) and following the instructions of the Luciferase Assay Kit (Promega, Madison, WI, USA). Protein concentration was measured by the Bradford assay (Bio-Rad). The background obtained with the lysis buffer was subtracted in each experimental value and the specific transactivation expressed as a fold induction over untreated cells. All the experiments were repeated at least 3 times. Rosiglitazone was purchased from Cayman Chemical Company (Ann Arbor, MI, USA) and used as a positive control in these *in vitro* experiments.

Statistics

Data were assessed by one- or two-way analysis of variance, as required, followed by the Student–Newman–Keuls test.

Results

Study of Neuroprotective Effects of CBG in 3NP-lesioned Mice

The intoxication of mice with 3NP resulted in a myriad of neurological, biochemical, and histological effects that were reminiscent of some aspects of HD pathology (reviewed in [22]). For example, 3NP-treated mice exhibited high scores in hindlimb clasping [$F_{(3,26)}=13.87$; $P<0.01$], dystonia [$F_{(3,26)}=10.55$; $P<0.01$], and in general locomotor activity [$F_{(3,26)}=18.742$; $P<0.01$] compared with control animals (Fig. 1). A similar tendency was seen for truncal dystonia, but it was not statistically significant (Fig. 1). In these animals, the administration of CBG improved the motor deficits typical of 3NP-lesioned mice by reducing hindlimb clasping and dystonia and general locomotor activity, but had no effect on trunkal dystonia (Fig. 1).

The striatal parenchyma of these 3NP-treated animals showed an important reduction in Nissl-stained cells [>50 %; $F_{(3,8)}=96.89$, $P<0.01$], which indicates an important degree of neuronal death caused by 3NP that was clearly prevented by treatment with CBG (Fig. 2). Neuronal cell death was confirmed by NeuN immunohistochemistry, which proved a reduction of about 50 % in the immunolabelling for this neuronal marker in the striatal parenchyma of 3NP-lesioned mice [$F_{(3,8)}=92.46$; $P<0.01$], which was paralleled by a notable increase in GFAP [$F_{(3,8)}=83.984$; $P<0.01$] and Iba-1 [$F_{(3,8)}=112.267$; $P<0.01$] immunostainings, indicating the occurrence of astrogliosis and reactive microgliosis, respectively (Fig. 3). NeuN immunostaining confirmed that CBG treatment prevented 3NP-induced neuronal loss (Fig. 3A). However, this treatment did not reduce the number of GFAP-positive cells, which, in fact, experienced an increase (Fig. 3B), and produced only a modest reduction in the reactive microgliosis (Iba-1-positive cells) (Fig. 3C). These observations were not unexpected as glial activation has been reported to be very poor after 3NP intoxication in rodents [6, 7, 14], oxidative injury and calpain activation being the key cytotoxic events underlying neuronal death in this experimental model [22].

As microglia activation and astrogliosis were barely or not affected by CBG, we were interested to investigate the mRNA expression of specific proinflammatory markers. We show that the expression of inflammatory enzymes, for example COX-2 [$F_{(3,8)}=29.071$; $P<0.01$ (Fig. 4A)] and iNOS [$F_{(3,8)}=34.051$; $P<0.01$ (Fig. 4D)], and the expression of proinflammatory cytokines, for example TNF-α [$F_{(3,8)}=53.869$; $P<0.01$ (Fig. 4B)] and IL-6 [$F_{(3,8)}=6.091$; $P<0.05$ (Fig. 4C)] were significantly upregulated in 3NP-lesioned mice. CBG significantly attenuated the upregulation of all the proinflammatory markers induced by 3NP (Fig. 4). Taken together, these results suggest that CBG mediates its anti-
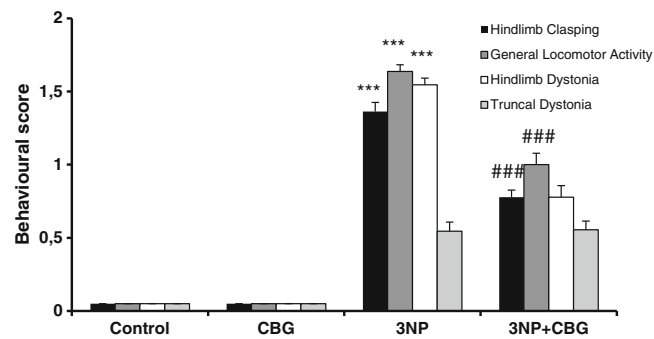
Fig. 1 Behavioral score after 3-nitropropionic acid (3NP) intoxication. Hindlimb clasping, general locomotor activity, hindlimb dystonia, and truncal dystonia were rated from 0 to 2 based on severity: a score of 0 typically indicates normal function and 2 indicates seriously affected function. Values are expressed as means ± SEM for 6–8 animals per group. Data were subjected to one-way analysis of variance followed by the Student–Newman–Keuls test. *$P<0.05$, **$P<0.01$, ***$P<0.001$ when comparing the control group with the 3NP group. #$P<0.05$, ##$P<0.01$, ###$P<0.001$ when comparing 3NP group with 3NP + cannabigerol (CBG) group

inflammatory activity on activated microglia and not in the signaling pathways that drive microglia cells from a resting state to an activated state.

Next, we used the striatum of 3NP-lesioned mice for analysis of some biochemical markers related to oxidative stress (e.g., catalase activity, SOD activity and GSH levels), which are particularly affected in this model [22]. As expected, there was a marked reduction in the activities of catalase [$F(3,8)=$ 12.593; $P<0.01$ (Fig. 5A)] and, in particular, SOD [$F(3,8)=$ 20.262; $P<0.01$ (Fig. 5C)], as well as in the levels of GSH [$F(3,8)=4.487$; $P<0.05$ (Fig. 5B)] compared with controls. CBG treatment recovered the activities of antioxidant enzymes, for example catalase, SOD-1, and the levels of GSH were reduced in the striatum of 3NP-intoxicated mice (Fig. 5). Collectively, these effects were compatible with an important neuroprotective effect exerted by CBG against the striatal
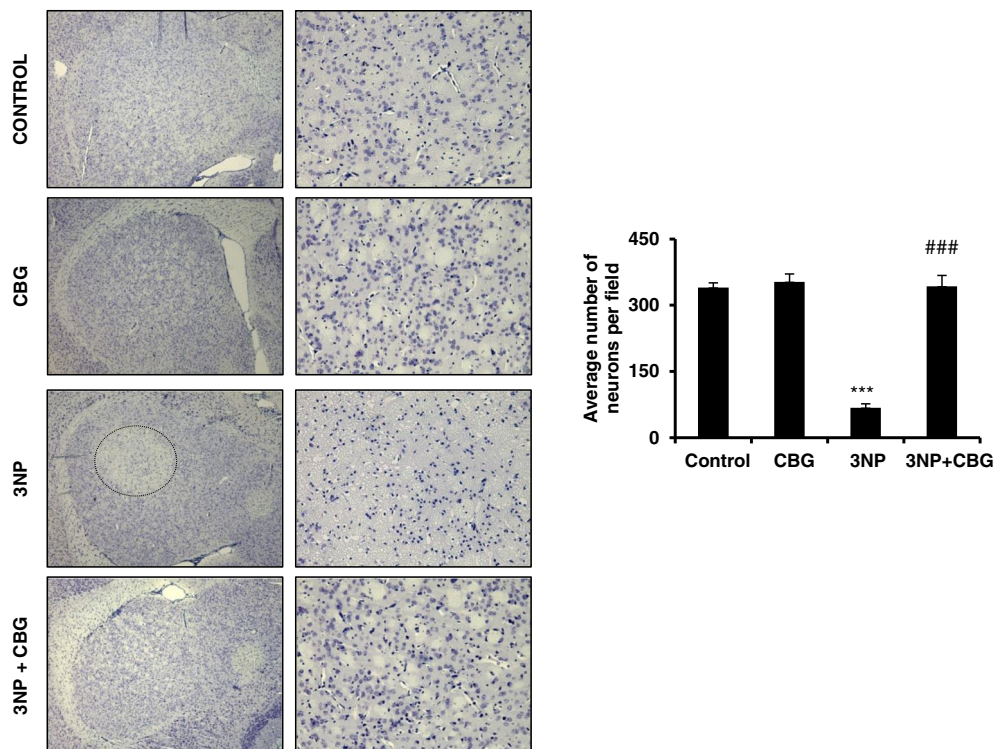
Fig. 2 Systemic administration of 3-nitropropionic acid (3NP) leads to a progressive and selective degeneration in the striatum. (Left) Cresyl violet staining was performed on brain sections from control, cannabigerol (CBG)-, 3NP-, and 3NP + CBG-treated mice. Low (left column) and high magnification (right column) showing the selective loss of cells in the striatum at day 5 (pale region, outlined). This lesion was not detectable in the group that received CBG. Images were acquired by using light microscopy. (Right) Quantification of Nissl-positive cells in the mouse striatum. Total average number of neurons (100× magnification) is shown. Values are expressed as means ± SEM for 6–8 animals per group. Data were subjected to one-way analysis of variance followed by the Student–Newman–Keuls test. ***$P<0.001$ when comparing the control group with the 3NP and CBG group. ###$P<0.001$ when comparing the 3NP group with the 3NP + CBG group

A) NeuN immunostaining

B) GFAP immunostaining

C) Iba-1 immunostaining
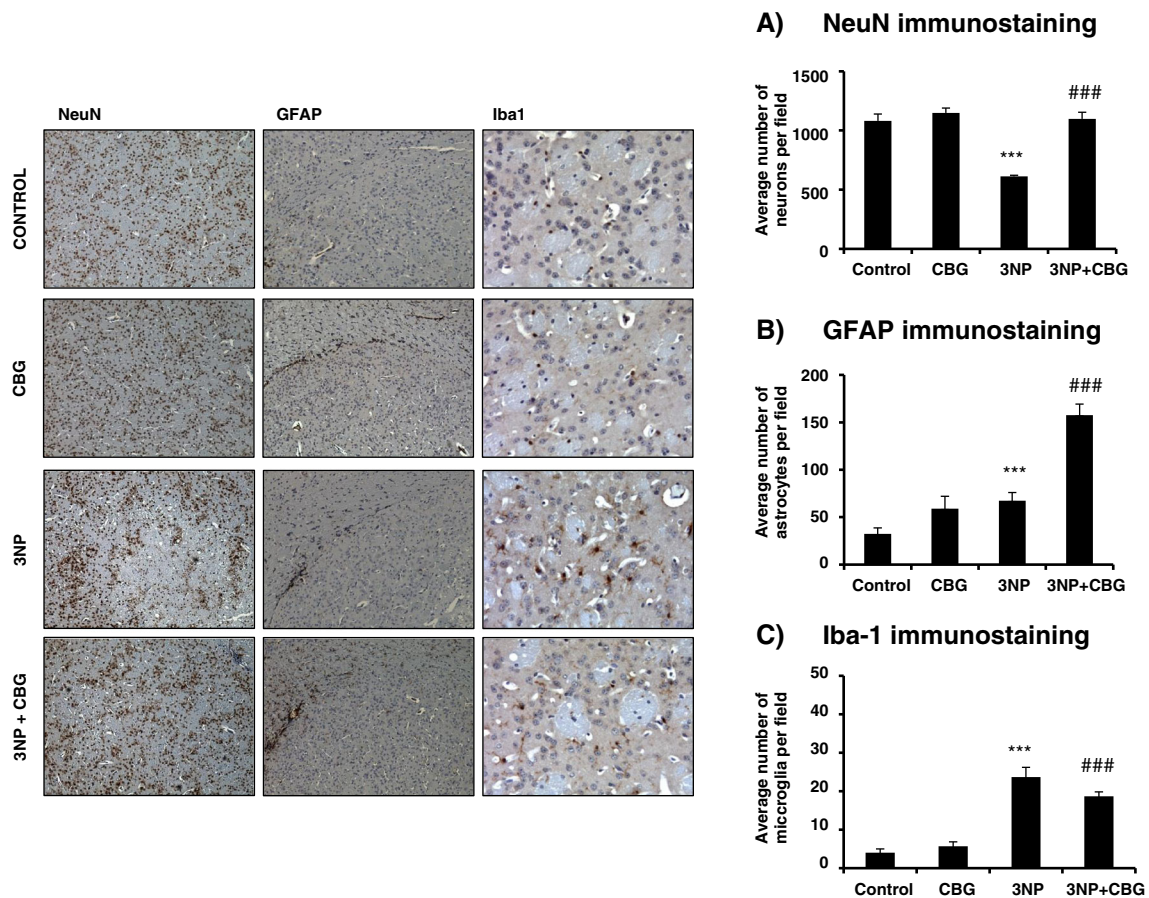
Fig. 3 (Left panels) Photomicrographs of NeuN (10×)-, glial fibrillary acidic protein (GFAP) (10×)-, and Iba1 (20×)-immunostained sections through the coronal section of striatum of control and 3-nitropropionic acid (3NP)-lesioned mice treated with vehicle or cannabigerol (CBG). They show a significant loss of NeuN-positive cells in the striatum of 3NP-treated mice compared with controls. CBG treatment significantly reduced 3NP-induced loss of striatal NeuN-positive cells. (Right panels) Quantification of (**A**) NeuN-, (**B**) GFAP-, and (**C**) Iba1-positive cells in the mouse striatum. Total average number of neurons, astrocytes (100× magnification) and microglia (200× magnification) is shown. Values are expressed as means ± SEM for 6–8 animals per group. Data were subjected to one-way analysis of variance followed by the Student–Newman–Keuls test. $*P<0.05$, $**P<0.01$, $***P<0.001$ when comparing the control group with the 3NP and CBG group. $^{\#}P<0.05$, $^{\#\#}P<0.01$, $^{\#\#\#}P<0.001$ when comparing the 3NP group with the 3NP + CBG group

damage caused by 3NP, which is also supported by the fact that the phytocannabinoid was mostly inactive on these parameters when it was administered to nonlesioned control animals (Figs 1–5).

Lastly, cDNA samples obtained from the striatum of animals lesioned with 3NP, their controls, and the 3NP-lesioned mice that were treated with CBG were analyzed with a specific HD array that measured the mRNA expression of 84 genes related to HD (Table S1; see Supplementary Information). Our purpose was to identify possible genes that, being affected by 3NP insult reproducing the changes observed in the human pathology, may be normalized by treatment with CBG. Using this HD RT-PCR panel, we found only 2 genes, *Cd44* and *Sgk1*, to be significantly upregulated (>2-fold induction or repression). *Cd44* was induced in 3NP mice compared with control mice (3.0-fold induction) and was significantly downregulated in 3NP mice treated with CBG (−1.3-fold repression). *Sgk1* was induced in 3NP mice compared

with control mice (2.7-fold induction) and was also significantly downregulated in 3NP mice treated with CBG (−1.41-fold repression). Although, in general, these results confirm that the molecular mechanisms underling HD physiopathology are quite different in 3NP and R6/2 murine models (see below), previous studies have confirmed the relation of these two genes with HD and other neuroinflammatory disorders [31, 32].

Study of Neuroprotective Effects of CBG in R6/2 Mice

We also investigated the neuroprotective properties of CBG in a transgenic murine model of HD, the R6/2 mice, which exhibit a very aggressive pathological phenotype that recapitulates most of the cytotoxic mechanisms that operate in the human pathology. Thus, compared with wild-type animals, R6/2 mice exhibited a characteristic loss of weight that was initiated at 8 weeks of age and that worsened at 10 weeks of

Fig. 4 Gene expression of inflammatory markers including (A) cyclooxygenase (COX)-2, (B) tumor necrosis factor (TNF)-α, (C) interleukin (IL)-6, and (D) inducible nitric oxide synthase (iNOS) was significantly downregulated in 3-nitropropionic acid (3NP) + cannabigerol (CBG)-treated mice compared with 3NP mice. Values are expressed as means ± SEM for 6–8 animals per group. Data were subjected to one-way analysis of variance followed by the Student–Newman–Keuls test. *$P<0.05$, **$P<0.01$, ***$P<0.001$ indicates significant changes between controls and 3NP mice. #$P<0.05$, ##$P<0.01$ indicates significant changes between 3NP- and 3NP + CBG-treated mice
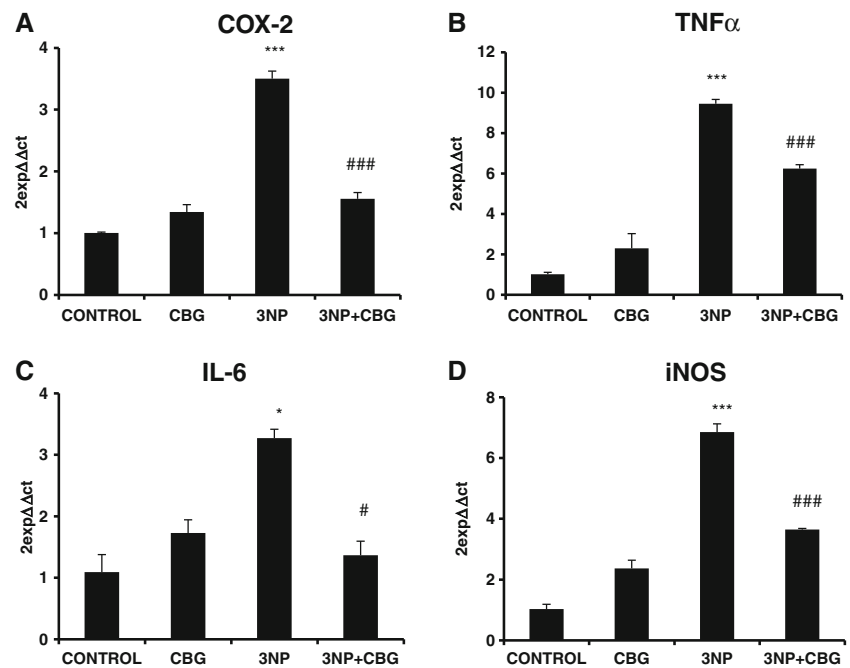
age when the animals were euthanized [$F(15,180)=12.13$; $P<0.01$ (Fig. 6A)]. This loss of weight has been largely reported in R6/2 mice and also in other transgenic models of HD [7–9, 14]. Treatment with CBG was not effective in recovering the characteristic loss of weight of R6/2 mice; it produced an apparent worsening effect (Fig. 6A). In parallel to the weight loss, R6/2 mice exhibited a deterioration in rotarod performance that was already evident at the age of 5 weeks, then occurring before the loss of weight, and that reached a maximum at 9 weeks after birth [$F(15,180)=4.208$; $P<0.01$), 1 week before animals were euthanized (Fig. 6B). The administration of CBG produced a modest recovery in this deteriorated rotarod performance, as revealed the fact that the time in the rod of R6/2 mice treated with CBG was always higher at all time points analyzed compared with R6/2 mice treated with vehicle (Fig. 6B). However, these differences were not statistically significant, being evident only because of a different probability level

for both groups compared with wild-type animals at specific time points, for example 8 weeks (Fig. 6B).

The analysis of the postmortem striatum of R6/2 animals at 10 weeks after birth proved important changes in specific markers of HD pathology, in particular, a profound reduction in the expression of CB$_1$ [$F(3,29)=22.50$; $P<0.01$ (Fig. 7A)], as has been largely demonstrated in patients with HD [33], and in this and other experimental models of HD [8, 14]. Upregulatory responses of CB$_2$ have been also found in previous studies [9, 10], and were also evident here, but to a significantly lesser extent [$F(3,26)=3.079$; $P<0.05$ (Fig. 7B)], and the same happened with expression of FAAH, which only showed a nonsignificant trend towards a decrease [$F(3,29)=1.208$; Fig. 7C), and therefore a much more moderate reduction than in previous studies in patients with HD [34]. However, the expression of MAGL had not previously been studied in R6/2 mice or other HD models, and proved to have a marked downregulatory response [$F(3,29)=23.02$; $P<0.01$
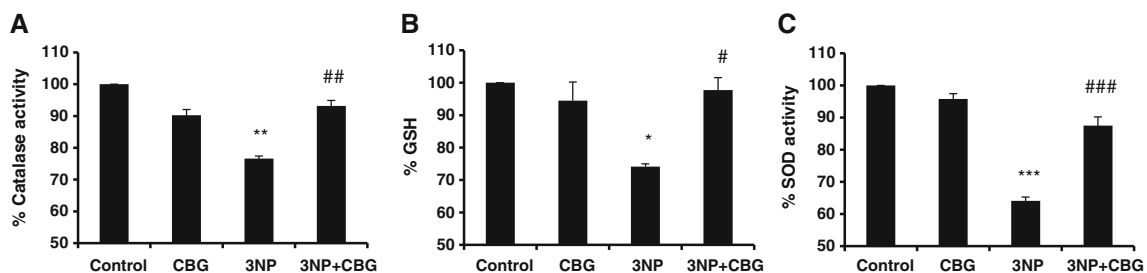

Fig. 5 Effect of cannabigerol (CBG) on antioxidant defenses in the striatum of 3-nitropropionic acid (3NP)-treated and control mice. Estimation of (A) catalase activity, (B) reduced glutathione (GSH) levels, and (C) superoxide dismutase (SOD) activity. Data presented are the percentage of the vehicle-treated control group and are expressed as means ± SEM for 6–8 animals per group. Data were subjected to one-way analysis of variance followed by the Student–Newman–Keuls test. *$P<0.05$, **$P<0.01$, ***$P<0.001$ when comparing the control group with the 3NP and CBG group. #$P<0.05$, ##$P<0.01$, ###$P<0.001$ when comparing the 3NP group with the 3NP + CBG group

Fig. 6 (**A**) Weight gain and (**B**) rotarod performance in R6/2 mice treated from the age of 4 weeks with cannabigerol (CBG) or vehicle (Tween 80-saline). Values are expressed as means ± SEM for 6–8 animals per group. Data were subjected to one-way analysis of variance followed by the Student–Newman–Keuls test (*$P<0.05$, **$P<0.01$, ***$P<0.005$ compared with wild-type animals treated with vehicle)
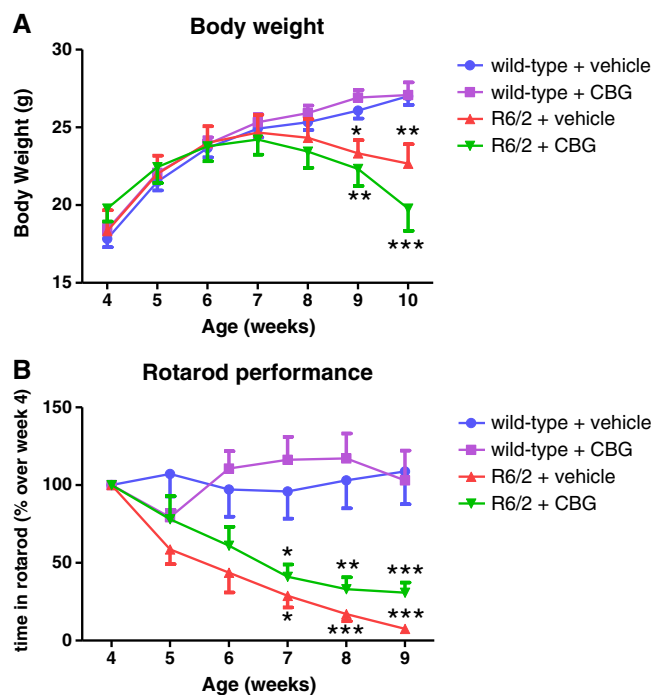
(Fig. 7D)]. Treatment with CBG only affected the gene expression for CB_2 with a small effect, which is reflected in the loss of statistical significance for the differences observed between wild-type animals and R6/2 mice when these mice were treated with CBG (Fig. 7B).

We also found the expected responses in R6/2 for other biochemical markers according to previous studies [8, 9, 35], for example in the neurotrophins BDNF and IGF-1, the expression of which experienced in both cases showed a dramatic reduction [BDNF: $F_{(3,28)}=5.618$ ($P<0.05$); IGF-1: $F_{(3,29)}=6.42$ ($P<0.05$) (Fig. 8A, B)], as previously described [2, 8]. Treatment with CBG partially improved deficits in both BDNF (Fig. 8A) and IGF-1 (Fig. 8B), but the effects were modest and similar to the case of CB_2 (e.g., loss of statistical significance of the differences observed between wild-type animals and R6/2 mice). R6/2 mice also exhibited deficits in the glial glutamate transporters GLAST [$F_{(3,31)}=11.44$; $P<0.01$ (Fig. 8D)] and, in particular, GLT-1 [$F_{(3,31)}=27.85$; $P<0.01$ (Fig. 8C)], also in accordance with previous data [36], but, in this case, there was no recovery by the treatment with CBG (Fig. 8C, D).

We also quantified DARPP-32, a protein involved in dopaminergic receptor signaling in striatal projection neurons, which experienced a dramatic reduction in gene expression [$F_{(3,31)}=18.79$; $P<0.01$ (Fig. 9A)] and immunostaining [$F_{(3,18)}=11.09$; $P<0.05$; Fig. 9B)] in R6/2 mice, concordant with the expected death of these neurons, and similar to previous studies [37]. None of these reductions was reversed by the treatment with CBG (Fig. 9A, B). We also found changes in inflammation-related markers such as the PPARγ receptors, which were downregulated in R6/2 mice [$F_{(3,25)}=$

4.32; $P<0.05$ (Fig. 9C)], and the cytokine TNF-α, which experienced a marked increase [$F_{(3,23)}=5.716$; $P<0.01$ (Fig. 9D)], in agreement with previous studies [38]. However, we did not find any changes in other proinflammatory parameters, such as the enzymes COX-2 or iNOS, and the cytokine IL-1β (data not shown), although this lack of response has been documented in the literature [39]. Treatment with CBG partially reversed the downregulation of PPARγ in R6/2 mice (Fig. 9C), being less effective against the increase in TNF-α, although a certain trend towards an attenuation may be appreciated in this parameter (Fig. 9D). In parallel to the increase in PPARγ expression by CBG in these mice, we also found that this phytocannabinoid dose-dependently activated PPARγ in cultured striatal cells expressing endogenous wild-type and mutant huntingtins (Figure S1; see Supplementary Information).

We were able to detect the presence of immunoreactivity for mutant huntingtin aggregates, labeled with EM48 antibody, in the striatal parenchyma of R6/2 mice (Fig. 10), although our immunohistochemical analysis with GFAP and Iba-1 did not reveal a marked glial activation (data not shown), as found in some studies [40]. Interestingly, EM48 immunostaining was slightly, but significantly, reduced in R6/2 mice treated with CBG (Fig. 10). Given that the number of striatal neurons does not appear to be significantly altered by treatment with CBG in R6/2 mice, according to the data obtained for DARPP-32 immunostaining (Fig. 9b), we believe that the reduction in EM48 immunostaining by CBG does not reflect a reduction in the number of neurons but a decrease in the number of mutant huntingtin aggregates in surviving neurons, which may be a beneficial event.

Fig. 7 Gene expression for (**A**) cannabinoid receptor type 1 (CB₁) and (**B**) cannabinoid receptor type 2 (CB₂) receptors, and (**C**) fatty acid hydrolase (FAAH) and (**D**) monoacylglycerol lipase (MAGL) measured in the striatum of R6/2 mice (10 weeks after birth) treated from the age of 4 weeks with cannabigerol (CBG) or vehicle (Tween 80-saline). Values correspond to fold of change over wild-type animals and are expressed as means ± SEM for 6–8 animals per group. Data were subjected to one-way analysis of variance followed by the Student–Newman–Keuls test (*$P<0.05$, **$P<0.01$, ***$P<0.005$ compared with wild-type animals treated with vehicle)
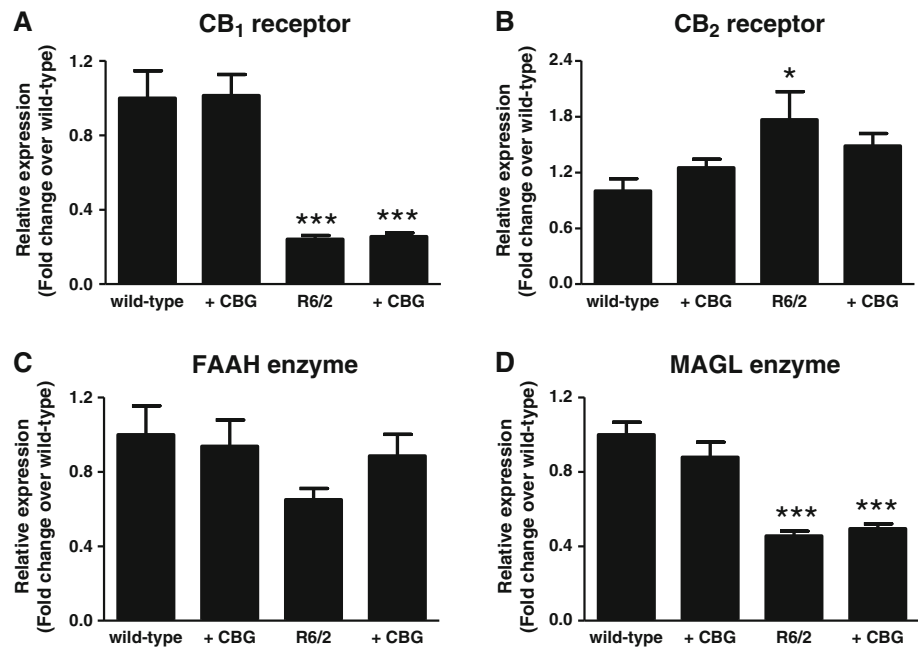
We also used the cDNA samples obtained from the striatum of R6/2 mice, their controls, and the transgenic mice that were treated with CBG for analysis with a specific HD array. Again, our purpose was to identify possible genes that, being affected in R6/2 mice reproducing more accurately the changes observed in the human pathology, may be normalized by treatment with CBG. We found numerous genes up- or down-regulated in R6/2 mice (Table S2; see Supplementary Information), but 7 that have been frequently linked to this disease given their role in the regulation of gene transcription (e.g., symplekin, Sin3a, Rcor1, histone deacetylase 2, and

huntingtin-associated protein 1), GABA transmission (e.g. δ subunit of the GABA-A receptor), and calcium homeostasis (e.g. hippocalcin), were found to be up- or down-regulated in R6/2 mice (Fig. 11A), as has previously been found in patients with HD or experimental models [41–44]. Importantly, the expression of these 7 genes was partially normalized by treatment with CBG (Fig. 11B), with some cases, for example huntingtin-associated protein 1, the increase found in R6/2 mice being completely reversed by CBG and exhibiting even lower expression levels than wild-type animals (Fig. 11B).

Fig. 8 Gene expression for (**A**) brain-derived neurotrophic factor (BDNF), (**B**) insulin-like growth factor (IGF)-1, (**C**) glutamate transporter (GLT)-1, and (**D**) glutamate aspartate transporter (GLAST) measured in the striatum of R6/2 mice (10 weeks after birth) treated from the age of 4 weeks with cannabigerol (CBG) or vehicle (Tween 80-saline). Values correspond to fold of change over wild-type animals and are expressed as means ± SEM for 6–8 animals per group. Data were subjected to one-way analysis of variance followed by the Student–Newman–Keuls test (*$P<0.05$, **$P<0.01$, ***$P<0.005$ compared with wild-type animals treated with vehicle)
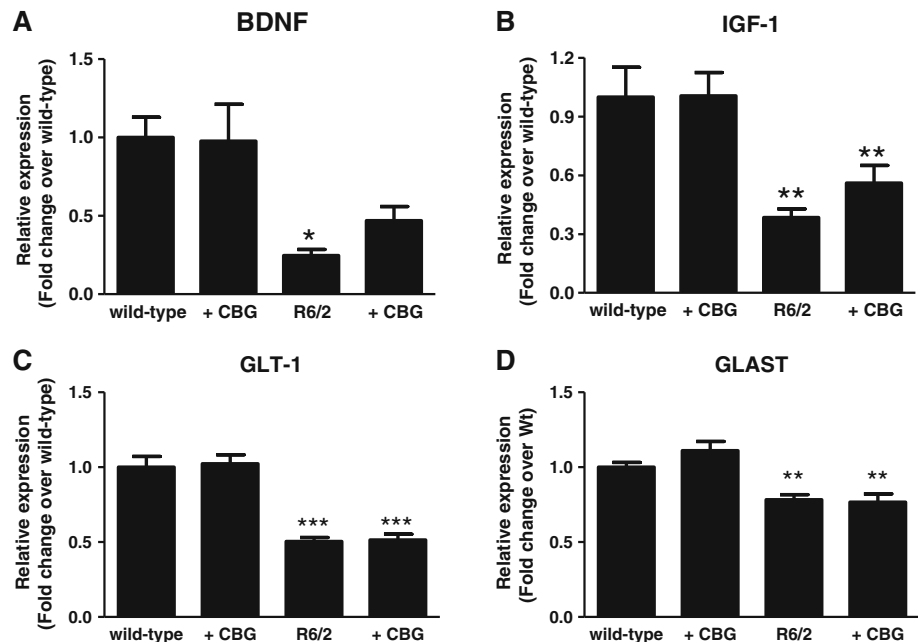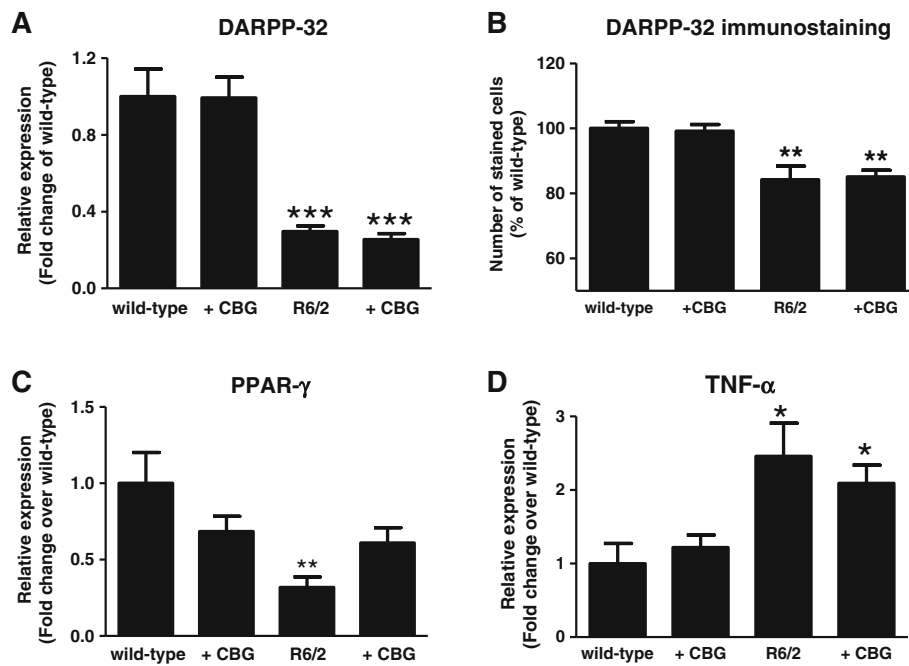
Fig. 9 Gene expression for (**A**) dopamine- and cyclic adenosine monophosphate-regulated phosphoprotein, Mr 32 kDA (DARPP-32), (**C**) peroxisome proliferator-activated receptor (PPAR)γ, and (**D**) tumour necrosis factor (TNF)-α, and (**B**) DARPP-32 immunostaining measured in the striatum of R6/2 mice (10 weeks after birth) treated from the age of 4 weeks with cannabiger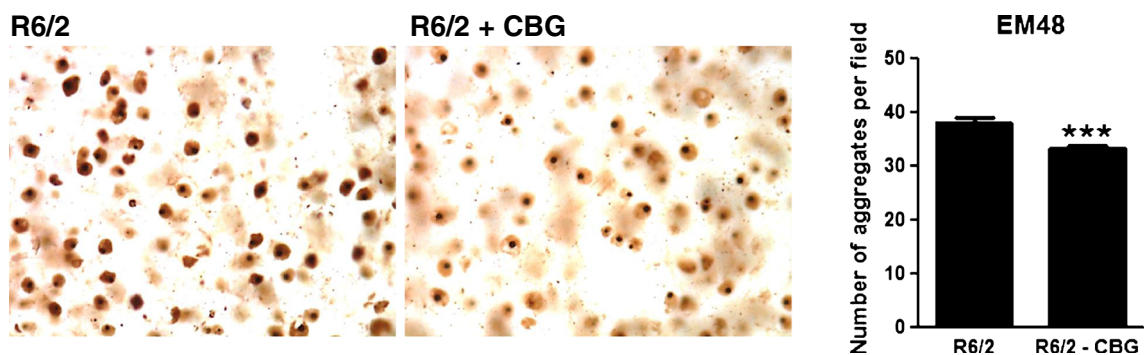ol (CBG) or vehicle (Tween 80-saline). Values correspond to fold of change (gene expression) or percentage (immunostaining) over wild-type animals and are expressed as means ± SEM for 6–8 animals per group. Data were subjected to one-way analysis of variance followed by the Student–Newman–Keuls test (*$P<0.05$, **$P<0.01$, ***$P<0.005$ compared with wild-type animals treated with vehicle)

Discussion

Only a few clinical studies have been performed to determine whether cannabinoid compounds are efficacious in HD, and the results they have yielded are rather controversial [45–48]. Possibly, the reason for such controversy is that these clinical studies concentrated more on HD symptoms rather than on disease progression. However, recent animal studies have demonstrated that combinations of different cannabinoids or the use of a broad-spectrum cannabinoid may delay disease progression by preserving striatal neurons from death in different animal models of HD, thus stressing the need for new clinical studies directed at testing whether the neuroprotective effects that certain cannabinoids induce in experimental models of HD are also reproduced in patients with HD [7–11]. This includes the evaluation of Δ^9-THC and CBD, separately or in a combination [6–9], Sativex®, which has been found to be neuroprotective in different animal models of HD [14, 49], and additional phytocannabinoids.

We were particularly interested in investigating whether CBG, another major phytocannabinoid present in *Cannabis sativa*, could be as effective a disease-modifying agent in HD. We studied its effects in 2 experimental models of HD, and found particularly positive results in the 3NP-lesioned mice model, a model in which the death of striatal neurons is dependent on mitochondrial damage, activation of calpain,

Fig. 10 EM48 immunostaining (representative of mutant huntingtin aggregates) in the striatum of R6/2 mice (at 10 weeks after birth) treated from the age of 4 weeks with cannabigerol (CBG) or vehicle (Tween 80-saline). The stainings were repeated in 5–6 animals per group. Magnification=40×. Data were subjected to Student's *t* test (***$P<0.005$ compared with R6/2 mice treated with vehicle)

A   **R6/2 vs wild-type**   **B**   **R6/2+CBG vs wild-type**
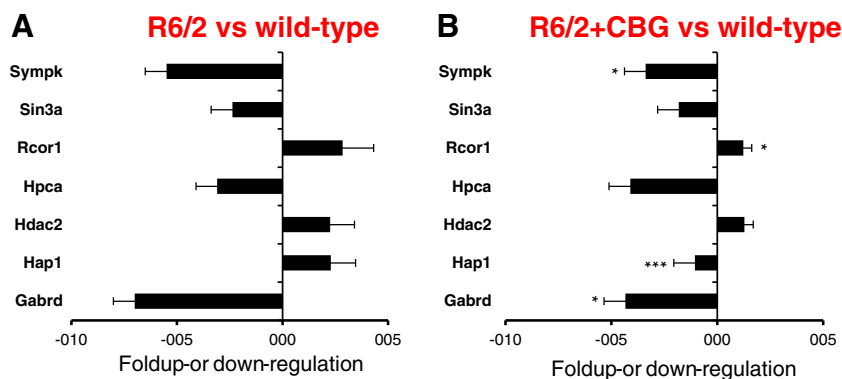
Fig. 11 Huntingdon's disease (HD) array analysis showing the up- or downregulatory responses of some genes specifically affected in the striatum of (**A**) R6/2 compared with wild-type mice or (**B**) R6/2 mice treated with CBG compared with wild-type mice. One microgram of RNA was retrotranscribed and the resulting cDNA was analyzed in a mouse HD polymerase chain reaction array. Five housekeeping genes contained on the experimental system were used to standardize the mRNA expression levels in every sample. Values correspond to number of folds that a specific gene is up- or downregulated. Data were assessed by the unpaired two-tailed Student's *t* test. The 7 genes presented in (A) were selected because the up- and downregulatory responses found between R6/2 and wild-type mice were more than 2-fold higher, and these differences were statistically significant in all cases, and also because these differences were reversed by the treatment with cannabigerol (CBG) (*$P<0.05$, **$P<0.01$, ***$P<0.005$)

and the generation of reactive oxygen species [14, 22]. In this model, subchronic administration of CBG preserved striatal neurons from 3NP-induced death presumably by regulating pro-oxidant and proinflammatory responses induced by 3NP intoxication. Importantly, the preservation of striatal neurons and the improvement of their homeostasis by CBG resulted in a significant improvement in the neurological deterioration typical of this model. These positive effects found in the 3NP model of HD were also investigated in a transgenic model of this disorder, the R6/2 mice, although the effects of CBG were much more modest in this model compared with the 3NP-lesioned mice. The most important observations in R6/2 mice were obtained from the analysis of the neurotrophins BDNF and IGF-1, and the PPARγ receptors, the deficits of which are strongly indicative of the deterioration in the striatal function—deficits that were partially reversed by CBG. We also collected some evidence from the data obtained with a specific HD array analysis, which showed some important HD-related genes, the up- or downregulatory responses of which were significantly attenuated by the treatment with CBG. Both types of responses are strongly associated with patients with HD in whom BDNF deficiency and alterations in symplekin [2], Sin3a, Rcor1, histone deacetylase 2, huntingtin-associated protein 1, and other genes related to the regulation of gene transcription have been found to play a key role in HD pathogenesis [41–44]. The presence of mutant huntingtin aggregates in the striatal parenchyma of R6/2 mice, another key event in human HD pathogenesis, was slightly reduced by CBG in these mice. By contrast, we did not obtain any evidence that CBG may preserve striatal neurons from death in R6/2 mice, as revealed by DARPP-32 immunostaining, but this fact appears to support the fact that the reduction in the number of mutant huntingtin aggregates reflects a lower presence of these aggregates in surviving neurons rather than a reduction due to lower number of striatal neurons. Reduction in huntingtin aggregation has been associated with a better striatal function, and has been proposed as a therapeutic objective in this disease [3].

In this study, we have not addressed the potential mechanisms involved in the beneficial effects of CBG in both HD models, something that will be done in follow-up studies. It is important to note that the profile of CBG has been poorly studied in relation to its therapeutic and pharmacological effects and, in particular, to its mechanisms of action, which makes it difficult to relate the effects found to specific targets and signaling pathways. However, we assume that the effects are not dependent on the activation of CB_1 and/or CB_2, given the poor affinity of CBG for these classic cannabinoid receptors [17, 18]. Like Δ^9-THC and CBD, CBG also penetrates the blood–brain barrier after i.p. delivery [50], and may target α-2 adrenergic receptors and PPARγ receptors in the brain [19, 21]. It has been shown that the expression of α-2 adrenergic receptors is increased in the hypothalamus of transgenic rats for HD [51], but antagonism rather than agonism is involved α-2 adrenergic receptor-mediated neuroprotection [52], and therefore it is unlikely that CBG alleviates HD symptoms and disease markers by targeting this receptor. On the contrary, PPARγ agonists such as thioglitazones have been shown to have a neuroprotective effect in *in vitro* and *in vivo* models of HD [53–55]. There is strong evidence that mitochondrial dysfunction results in neurodegeneration and may contribute to the pathogenesis of HD. Studies over the last few years have implicated an impaired function of PPARγ co-activator-1α (PGC-1α), a master co-regulator of mitochondrial biogenesis, metabolism, and antioxidant defenses, in causing mitochondrial dysfunction in HD. PPARγ agonists are neuroprotective, increase oxidative phosphorylation capacity in mouse and human cells, and

enhance mitochondrial function [56]. In addition, it has also been demonstrated that oral treatment with rosiglitazone induced mitochondrial biogenesis in mouse brain [57]. Therefore, we assume that the activation of PPARγ receptors may be certainly the most feasible mechanism for CBG effects in HD, in particular in 3NP-lesioned mice, although this would need to be demonstrated in follow-up studies. We also consider that these nuclear receptors may be also involved in the effects of CBG in R6/2 mice. In support of this hypothesis, we have found that CBG activated PPARγ in striatal cells expressing endogenous wild-type and mutant huntingtins, an experimental condition relatively comparable with the case of R6/2 mice. However, low levels of PPARγ receptors are expected in the striatum of these mice given their low levels of gene expression found in our study. In fact, these presumably reduced PPARγ receptor levels, together with the fact that CBG does not activate CB_1 and CB_2 and that, in R6/2 mice, the role of these receptors in mediating the neuroprotective effects of cannabinoids is much more relevant [8, 9], might explain that the effects found with CBG in R6/2 mice have been much more modest compared with 3NP-lesioned mice, suggesting the need to continue the studies in R6/2 mice using combinations of CBG with other phytocannabinoids.

However, substantial literature indicates that HD pathology develops via multiple pathways that may act synergistically. A recent report has investigated the gene expression profile in different animal models of HD compared with striatal gene expression phenotype of human HD [58]. In such a study, the authors found differences between the R6/2 and the 3NP models, showing that the 3NP profile is consistent with neuroinflammation, with changes in genes involved in immune response, response to wounding, defense response, and inflammatory response. In our study, with a limited number of HD-related genes, we also found clear differences between R6/2 (significant changes in 21 of 84 genes) and 3NP (significant changes in 3 of 84 genes) (see Supplementary Information) models. This result may be explained by the rapid induction of cell death mechanisms mediated by 3NP, and the array data may reflect only a small fraction of dysfunctional neurons present at one time. Thus, it will be interesting to study the effect of CBG on the profile of gene expression in 3NP-lesioned animals before the loss of striatal cells.

Finally, given that the improvement of antioxidant defenses by CBG, reflected in increased activities of catalase and SOD-1 and higher levels of GSH, appears to be a key mechanism for the beneficial effects of this phytocannabinoid in the 3NP model, we were also interested in investigating whether the neuroprotective effects of CBG in this pro-oxidant model may be associated with specific effects on Nrf-2 signaling and/or on the target genes for this transcription factor, a fact also proposed for the antioxidant effects of cannabidiol [15]. However, preliminary immunostaining of Nrf-2 and qRT-PCR analysis of Nrf-2-dependent genes failed to prove any effect of CBG at this level (data not shown).

In summary, CBG appears to have a promising neuroprotective profile for the treatment of HD, a fact already investigated with other phytocannabinoids separately or in combination [6–9, 14, 49]. CBG appears to be particularly active against the mitochondrial dysfunction, calpain activation and oxidative injury caused by 3NP. It was also active in R6/2 mice, but with only modest effect, so it is possible that it needs to be combined with another phytocannabinoid in these mice to enhance its therapeutic effects, in particular with cannabinoids having activity at CB_1 and/or CB_2 receptors, which have been found to serve as therapeutic targets in these mice [8, 9]. This additional investigation will be critical before proceeding to clinical studies with CBG in patients with HD.

References

1. Roze E, Bonnet C, Betuing S, Caboche J. Huntington's disease. Adv Exp Med Biol 2010;685:45–63.
2. Zuccato C, Valenza M, Cattaneo E. Molecular mechanisms and potential therapeutical targets in Huntington's disease. Physiol Rev 2010;90:905–981.
3. Johnson CD, Davidson BL. Huntington's disease: progress toward effective disease-modifying treatments and a cure. Hum Mol Genet 2010;19:R98-R102.
4. Pazos MR, Sagredo O, Fernández-Ruiz J. The endocannabinoid system in Huntington's disease. Curr Pharm Des 2008;14:2317–2325.
5. Fernández-Ruiz J, García C, Sagredo O, Gómez-Ruiz M, de Lago E. The endocannabinoid system as a target for the treatment of neuronal damage. Expert Opin Ther Targets 2010;14:387–404.
6. Lastres-Becker I, Bizat N, Boyer F, Hantraye P, Fernández-Ruiz J, Brouillet E. Potential involvement of cannabinoid receptors in 3-nitropropionic acid toxicity in vivo. Neuroreport 2004;15:2375–2379.
7. Sagredo O, Ramos JA, Decio A, Mechoulam R, Fernández-Ruiz J. Cannabidiol reduced the striatal atrophy caused 3-nitropropionic acid in vivo by mechanisms independent of the activation of cannabinoid, vanilloid TRPV1 and adenosine A2A receptors. Eur J Neurosci 2007;26:843–851.

8. Blázquez C, Chiarlone A, Sagredo O, et al. Loss of striatal type 1 cannabinoid receptors is a key pathogenic factor in Huntington's disease. Brain 2011;134:119–136.

9. Palazuelos J, Aguado T, Pazos MR, et al. Microglial CB2 cannabinoid receptors are neuroprotective in Huntington's disease excitotoxicity. Brain 2009;132:3152–3164.

10. Sagredo O, González S, Aroyo I, et al. Cannabinoid CB2 receptor agonists protect the striatum against malonate toxicity: relevance for Huntington's disease. Glia 2009;57:1154–1167.

11. Pintor A, Tebano MT, Martire A, et al. The cannabinoid receptor agonist WIN 55,212-2 attenuates the effects induced by quinolinic acid in the rat striatum. Neuropharmacology 2006;51:1004–1012.

12. Sastre-Garriga J, Vila C, Clissold S, Montalban X. THC and CBD oromucosal spray (Sativex®) in the management of spasticity associated with multiple sclerosis. Expert Rev Neurother 2011;11:627–637.

13. Zajicek JP, Apostu VI. Role of cannabinoids in multiple sclerosis. CNS Drugs 2011;25:187–201.

14. Sagredo O, Pazos MR, Satta V, Ramos JA, Pertwee RG, Fernández-Ruiz J. Neuroprotective effects of phytocannabinoid-based medicines in experimental models of Huntington's disease. J Neurosci Res 2011;89:1509–1518.

15. Fernández-Ruiz J, Sagredo O, Pazos MR, et al. Cannabidiol for neurodegenerative disorders: important new clinical applications for this phytocannabinoid? Br J Clin Pharmacol 2013;75:323–333.

16. O'Sullivan SE. Cannabinoids go nuclear: evidence for activation of peroxisome proliferator-activated receptors. Br J Pharmacol 2007;152:576–582.

17. Izzo AA, Borrelli F, Capasso R, Di Marzo V, Mechoulam R. Non-psychotropic plant cannabinoids: new therapeutic opportunities from an ancient herb. Trends Pharmacol Sci 2009;30:515–527.

18. Hill AJ, Williams CM, Whalley BJ, Stephens GJ. Phytocannabinoids as novel therapeutic agents in CNS disorders. Pharmacol Ther 2012;133:79–97.

19. Granja AG, Carrillo-Salinas F, Pagani A, et al. A cannabigerol quinone alleviates neuroinflammation in a chronic model of multiple sclerosis. J Neuroimmune Pharmacol 2012;7:1002–1016.

20. Borrelli F, Fasolino I, Romano B, et al. Beneficial effect of the non-psychotropic plant cannabinoid cannabigerol on experimental inflammatory bowel disease. Biochem Pharmacol 2013;85:1306–1316.

21. Cascio MG, Gauson LA, Stevenson LA, Ross RA, Pertwee RG. Evidence that the plant cannabinoid cannabigerol is a highly potent alpha2-adrenoceptor agonist and moderately potent 5HT1A receptor antagonist. Br J Pharmacol 2010;159:129–141.

22. Brouillet E, Jacquard C, Bizat N, Blum D. 3-Nitropropionic acid: a mitochondrial toxin to uncover physiopathological mechanisms underlying striatal degeneration in Huntington's disease. J Neurochem 2005;95:1521–1540.

23. Pouladi MA, Xie Y, Skotte NH, et al. Full-length huntingtin levels modulate body weight by influencing insulin-like growth factor 1 expression. Hum Mol Genet 2010;19:1528–1538.

24. Fernagut PO, Diguet E, Stefanova N, et al. Subacute systemic 3-nitropropionic acid intoxication induces a distinct motor disorder in adult C57Bl/6 mice: behavioural and histopathological characterisation. Neuroscience 2002;114:1005–1017.

25. Luck H. Catalase. In: Bergmeyer HU (ed.) Methods of enzyme analysis. Academic Press, New York, 1971, p. 885.

26. Kono Y. Generation of superoxide radical during autoxidation of hydroxylamine and and assay for superoxide dismutase. Arch Biochem Biophys 1978;186:189–195.

27. Ellman GL. Tissue sulfhydryl groups. Arch Biochem Biophys 1978;82:70–77.

28. Gray M, Shirasaki DI, Cepeda C, et al. Full-length human mutant huntingtin with a stable polyglutamine repeat can elicit progressive and selective neuropathogenesis in BACHD mice. J Neurosci 2008;28:6182–6195.

29. Alvarez FJ, Lafuente H, Rey-Santano MC, et al. Neuroprotective effects of the nonpsychoactive cannabinoid cannabidiol in hypoxic-ischemic newborn piglets. Pediatr Res 2008;64:653–658.

30. Trettel F, Rigamonti D, Hilditch-Maguire P, et al. Dominant phenotypes produced by the HD mutation in STHdh(Q111) striatal cells. Hum Mol Genet 2000;9:2799–2809.

31. Rangone H, Poizat G, Troncoso J, et al. The serum- and glucocorticoid-induced kinase SGK inhibits mutant huntingtin-induced toxicity by phosphorylating serine 421 of huntingtin. Eur J Neurosci 2004;19:273–279.

32. Tuohy TM, Wallingford N, Liu Y, et al. CD44 overexpression by oligodendrocytes: a novel mouse model of inflammation-independent demyelination and dysmyelination. Glia 2004;47:335–345.

33. Glass M, Dragunow M, Faull RL. The pattern of neurodegeneration in Huntington's disease: a comparative study of cannabinoid, dopamine, adenosine and GABA(A) receptor alterations in the human basal ganglia in Huntington's disease. Neuroscience 2000;97:505–519.

34. Battista N, Bari M, Tarditi A, et al. Severe deficiency of the fatty acid amide hydrolase (FAAH) activity segregates with the Huntington's disease mutation in peripheral lymphocytes. Neurobiol Dis 2007;27:108–116.

35. Apostol BL, Simmons DA, Zuccato C, et al. CEP-1347 reduces mutant huntingtin-associated neurotoxicity and restores BDNF levels in R6/2 mice. Mol Cell Neurosci 2008;39:8–20.

36. Estrada-Sánchez AM, Montiel T, Segovia J, Massieu L. Glutamate toxicity in the striatum of the R6/2 Huntington's disease transgenic mice is age-dependent and correlates with decreased levels of glutamate transporters. Neurobiol Dis 2009;34:78–86.

37. Luthi-Carter R, Strand A, Peters NL, et al. Decreased expression of striatal signaling genes in a mouse model of Huntington's disease. Hum Mol Genet 2000;9:1259–1271.

38. Crocker SF, Costain WJ, Robertson HA. DNA microarray analysis of striatal gene expression in symptomatic transgenic Huntington's mice (R6/2) reveals neuroinflammation and insulin associations. Brain Res 2006;1088:176–186.

39. Deckel AW, Gordinier A, Nuttal D, et al. Reduced activity and protein expression of NOS in R6/2 HD transgenic mice: effects of L-NAME on symptom progression. Brain Res 2001;919:70–81.

40. Yu ZX, Li SH, Evans J, Pillarisetti A, Li H, Li XJ. Mutant huntingtin causes context-dependent neurodegeneration in mice with Huntington's disease. J Neurosci 2003;23:2193–2202.

41. Zucker B, Luthi-Carter R, Kama JA, et al. Transcriptional dysregulation in striatal projection- and interneurons in a mouse model of Huntington's disease: neuronal selectivity and potential neuroprotective role of HAP1. Hum Mol Genet 2005;14:179–189.

42. Jovicic A, Zaldivar Jolissaint JF, Moser R, Silva Santos Mde F, Luthi-Carter R. MicroRNA-22 (miR-22) overexpression is neuroprotective via general anti-apoptotic effects and may also target specific Huntington's disease-related mechanisms. PLOS ONE 2013;8:e54222.

43. Mielcarek M, Benn CL, Franklin SA, et al. SAHA decreases HDAC 2 and 4 levels in vivo and improves molecular phenotypes in the R6/2 mouse model of Huntington's disease. PLOS ONE 2011;6:e27746.

44. Rudinskiy N, Kaneko YA, Beesen AA, et al. Diminished hippocalcin expression in Huntington's disease brain does not account for increased striatal neuron vulnerability as assessed in primary neurons. J Neurochem 2009;111:460–472.

45. Consroe P, Laguna J, Allender J, et al. Controlled clinical trial of cannabidiol in Huntington's disease. Pharmacol Biochem Behav 1991;40:701–708.

46. Curtis A, Rickards H. Nabilone could treat chorea and irritability in Huntington's disease. J Neuropsychiatry Clin Neurosci 2006;18:553–554.

47. Curtis A, Mitchell I, Patel S, Ives N, Rickards H. A pilot study using nabilone for symptomatic treatment in Huntington's disease. Mov Disord 2009;24:2254–2259.

48. Müller-Vahl KR, Schneider U, Emrich HM. Nabilone increases choreatic movements in Huntington's disease. Mov Disord 1999;14:1038–1040.

49. Valdeolivas S, Satta V, Pertwee RG, Fernández-Ruiz J, Sagredo O. Sativex-like combination of phytocannabinoids is neuroprotective in malonate-lesioned rats, an inflammatory model of Huntington's disease: role of CB1 and CB2 receptors. ACS Chem Neurosci 2012;3:400–406.

50. Deiana S, Watanabe A, Yamasaki Y, et al. Plasma and brain pharmacokinetic profile of cannabidiol (CBD), cannabidivarine (CBDV), Δ^9-tetrahydrocannabivarin (THCV) and cannabigerol (CBG) in rats and mice following oral and intraperitoneal administration and CBD action on obsessive-compulsive behaviour. Psychopharmacology (Berl) 2012;219:859–873.

51. Bode FJ, Stephan M, Wiehager S, et al. Increased numbers of motor activity peaks during light cycle are associated with reductions in adrenergic alpha(2)-receptor levels in a transgenic Huntington's disease rat model. Behav Brain Res 2009;205:175–182.

52. Martel J, Chopin P, Colpaert F, Marien M. Neuroprotective effects of the alpha2-adrenoceptor antagonists, (+)-efaroxan and (+/−)-idazoxan, against quinolinic acid-induced lesions of the rat striatum. Exp Neurol 1998;154:595–601.

53. Quintanilla RA, Jin YN, Fuenzalida K, Bronfman M, Johnson GV. Rosiglitazone treatment prevents mitochondrial dysfunction in mutant huntingtin-expressing cells: possible role of peroxisome proliferator-activated receptor-γ (PPAR-γ) in the pathogenesis of Huntington disease. J Biol Chem 2008;283:25628–25637.

54. Johri A, Calingasan NY, Hennessey TM, et al. Pharmacologic activation of mitochondrial biogenesis exerts widespread beneficial effects in a transgenic mouse model of Huntington's disease. Hum Mol Genet 2012;21:1124–1137.

55. Jin J, Albertz J, Guo Z, et al. Neuroprotective effects of PPAR-γ agonist rosiglitazone in N171-82Q mouse model of Huntington's disease. J Neurochem 2013;125:410–419.

56. Schütz B, Reimann J, Dumitrescu-Ozimek L, et al. The oral antidiabetic pioglitazone protects from neurodegeneration and amyotrophic lateral sclerosis-like symptoms in superoxide dismutase-G93A transgenic mice. J Neurosci 2005;25:7805–7812.

57. Strum JC, Shehee R, Virley D, et al. Rosiglitazone induces mitochondrial biogenesis in mouse brain. J Alzheimers Dis 2007;11:45–51.

58. Strand AD, Baquet ZC, Aragaki AK, et al. Expression profiling of Huntington's disease models suggests that brain-derived neurotrophic factor depletion plays a major role in striatal degeneration. J Neurosci 2007;27:11758–11768.